Supporting Information: Mechanisms of H and CO Loss from the Uracil Nucleobase Following Low Energy Electron Irradiation.

Mark A. Fennimore, Tolga N. V. Karsili and Spiridoula Matsika**

Temple University, Philadelphia, USA

Cartesian coordinates associated with the transition states and minimum-energy conical intersection are given in Section 1. Orbitals of the products are also shown.

The stabilization method used herein is described in Section 2 and presented for several representative geometries along Q_{CO}.

Section 3 compares the PE profiles obtained from CASPT2 and EOM-EA-CCSD.

Section 4 gives the coordinates of fragments depicted in Figure 3 of the manuscript.

1. Transition states and conical intersections

Table S1: xyz coordinates for transition state of neutral uracil along the CO elimination trajectory obtained at the DFT/B3LYP/6-31G(d) level.

Neutral Transition State Geometry [Angstrom]

Atom	x	y	z
N	0.000000	0.000000	0.000000
C	0.000000	0.000000	1.410621
H	0.917867	0.000000	1.980949
C	-1.221345	0.479450	1.802271
H	-1.415644	0.955128	2.757345
C	-2.600889	0.021415	1.109910
O	-3.758259	0.073084	1.338698
N	-1.755823	1.395470	0.430161
H	-2.033169	2.381235	0.343569
C	-0.841909	0.928026	-0.581715
O	-0.838477	1.306032	-1.734801
H	0.715385	-0.417596	-0.578866
H	0.715385	-0.417596	-0.578866

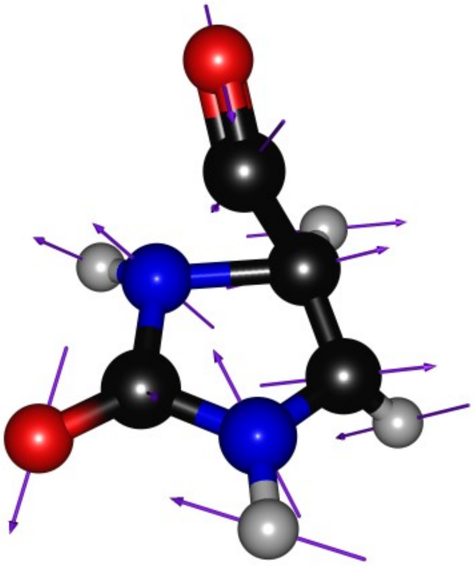

Figure S1: Structure and imaginary eigenvectors associated with the transition state en route to elimination via the neutral ground state.

Table S2: xyz coordinates for the anion optimized transition state of uracil along the CO elimination path obtained at the DFT/B3LYP/6-31G(d) level.

	Anion Optimized TS [Angstrom]		
	x	**y**	**z**
N	0.959005	0.931982	0.540244
C	-0.091171	1.514887	-0.257449
H	0.275633	2.100824	-1.117799
C	-0.887841	0.402240	-0.606615
H	-1.414544	0.412757	-1.567994
C	-1.746019	-0.166677	0.498815
O	-2.863179	-0.604307	0.382220
N	0.366407	-0.948412	-0.582617
H	0.668839	-1.647732	-1.257089
C	1.390605	-0.328607	0.062062
O	2.549083	-0.743220	0.261617
H	1.711514	1.498319	0.907922

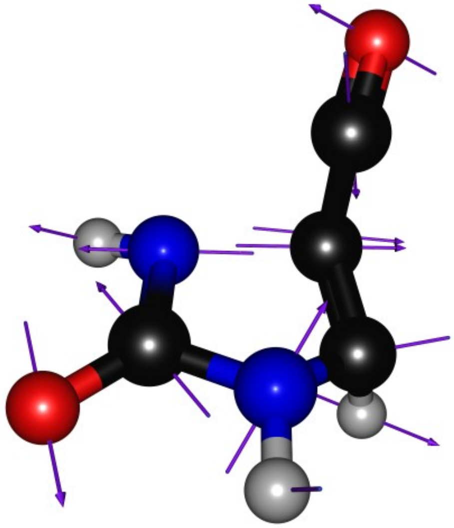

Figure S2: Structure and imaginary eigenvectors associated with the transition state en route to CO elimination via the anionic ground state.

Table S3: xyz coordinates for the D_0/D_1 conical intersection along the CO elimination trajectory obtained at the CASSCF(7,6)/6-31G(d) level.

	D_1/D_0 Conical Intersection [Angstrom]		
Atom	**X**	**y**	**z**
N	1.186516	0.988994	0.011606
C	-0.087379	1.523037	0.164948
H	-0.107950	2.603318	0.094293
C	-1.256725	0.827196	-0.368208
H	-1.585924	0.990017	-1.385785
C	-1.961454	-0.217540	0.372323
O	-2.952750	-0.811113	0.121618
N	0.482394	-1.199884	-0.253184
H	0.828610	-2.144600	-0.282302
C	1.508968	-0.409081	-0.026883
O	2.705144	-0.669648	0.134034
H	1.943288	1.531910	0.366546

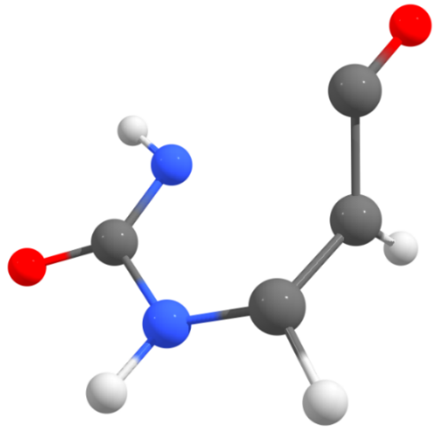

Figure S3: Structure of the D_0/D_1 CI along the CO elimination trajectory.

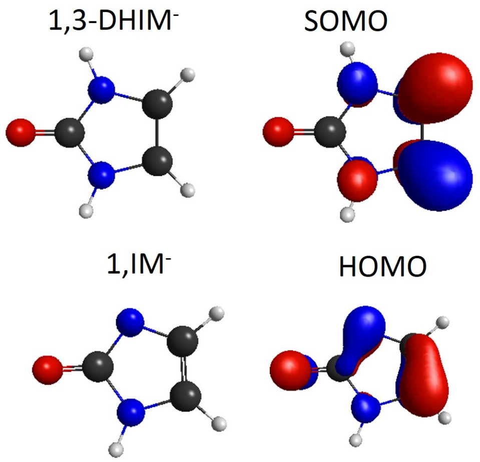

Figure S4: Orbitals of the intermediate and final product.

2. Stabilization curves

The energies and widths shown in Figure 5 of the manuscript are obtained using an orbital stabilization method on each geometry point. Stabilization curves for representative points are shown in Figures S5-S9. α is the parameter scaling the exponent of the diffuse functions in the basis set. X shows the position of the avoided crossings used in the analytic continuation procedure to extract the positions and widths.

Tables S4-S6 show the results of the analytic continuation as applied to each avoided crossing in each graph. Analytic Continuation can be used with the orbital stabilization method where the complex stationary points and energies are located using various forms of the Generalized Padé Approximation (GPA). GPA has been used here in two predominant forms—one in which the real energy is expanded as a quadratic and the other a cubic polynomial. [1-3]

$$E^2 P + E\,Q + R = 0 \qquad \text{Eq. } 1\alpha$$

$$E^3 P + E^2 Q + RE + S = 0 \qquad \text{Eq. } 2$$

The quantities, P, Q and R in Eq. 1 and S in Eq. 2 are themselves polynomial expansions of the scaling parameter (α) with coefficients p_i, r_k, q_j and s_l respectively. Equations 1 and 2 are commonly denoted as the (*i, j, k*) and (*i, j, k, l*) General Padé Approximations. As a matter of convention, the indices *i, j, k* and *l* are held equivalent to one another giving rise to 11, 14 and 17 unknowns for the (*3,3,3*), (*4,4,4*) and (*5,5,5*) approximations respectively. Similarly, the (*3,3,3,3*) GPA has 15 and the (*4,4,4,4*) 19 unknowns in p_i, r_k, q_j *and* s_l. These unknowns are found by fitting to the calculated energies.

$$P = 1 + \sum_{1}^{i} p_i \alpha^i \qquad R = \sum_{0}^{k} r_k \alpha^k \qquad Q = \sum_{0}^{j} q_j \alpha^j \qquad S = \sum_{0}^{l} s_l \alpha^l$$

Once P, R, Q and S (in the case of the cubic expansion) are known, the location of the complex stationary points (a*) may be determined by calculating the roots of the following equation

$$\frac{dE}{d\alpha} = 0$$

Once the stationary points are found they can be substituted back to Eq.1 and 2 to obtain the complex energies. In Tables S4-S6, results are shown for various GPA expansions, denoted as (3,3,3), (4,4,4), (5,5,5) and (4,4,4,4). The very minor variations in the returned solution serve as a confirmation of their validity. On the other hand, the results vary to a greater extent when derived from the distinct avoided crossings. This is a manifestation of the limited number of diffuse functions used.

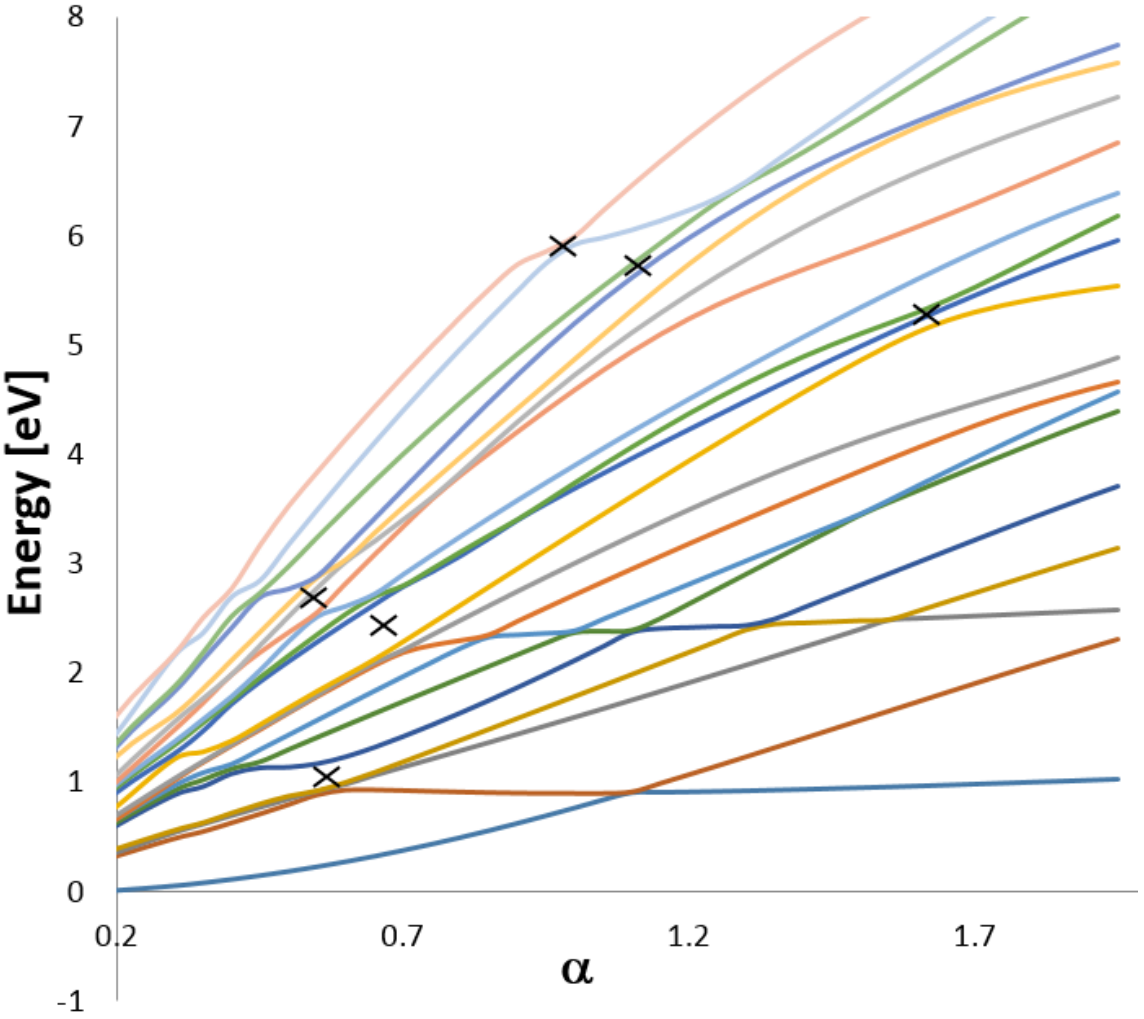

Figure S5: EOM-EA-CCSD/6-31+G* stabilization curve for the equilibrium geometry (Q_{CO}=0) of uracil. The stabilization curves were calculated in C1 symmetry.

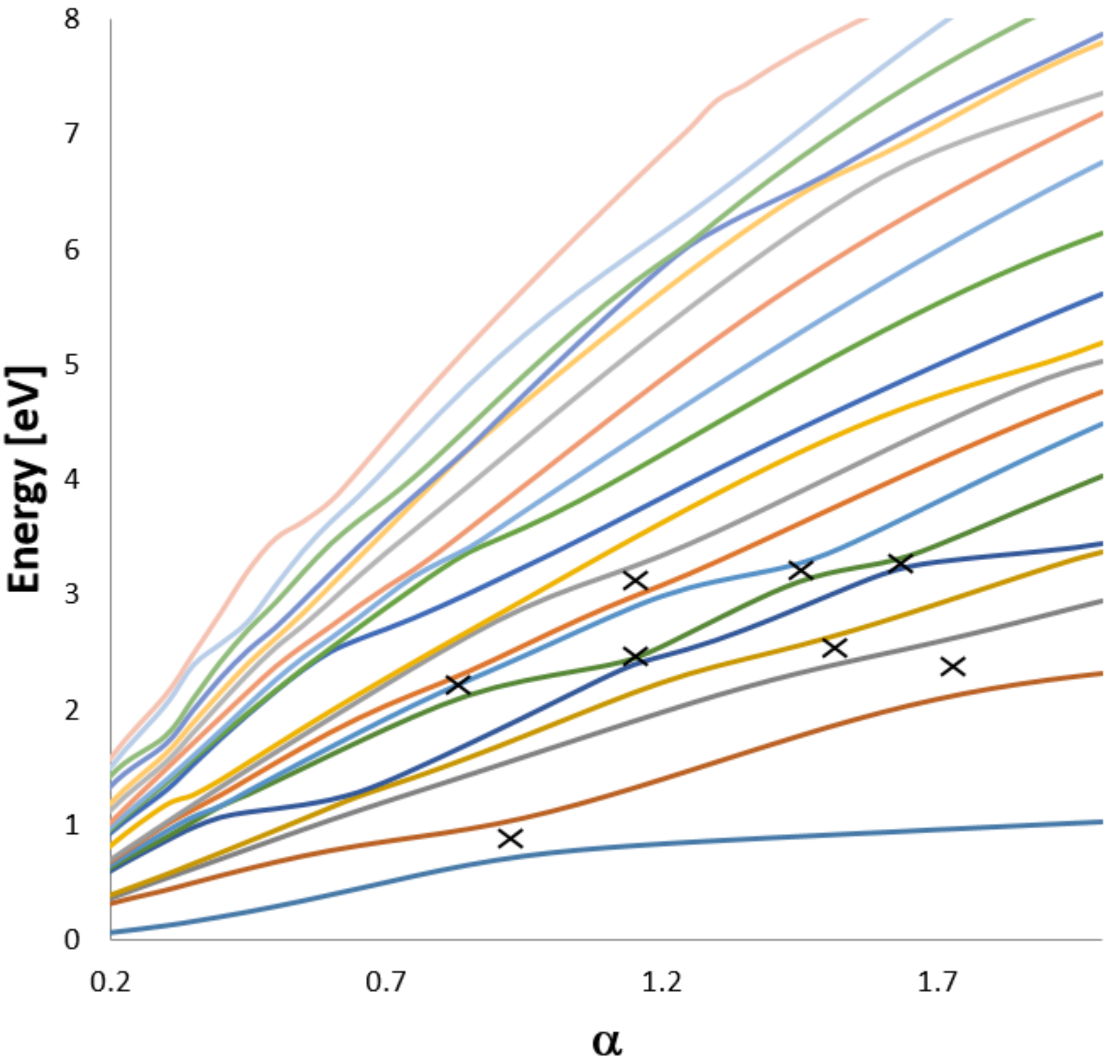

Figure S6: EOM-EA-CCSD/6-31+G* stabilization curve for Q_{CO}=0.4 along the CO elimination coordinate. The 3^2A” resonance is lower in energy here compared to Q_{CO}=0, and the interaction between the continuum solutions with the resonances are much more notable – leading to visually distinct avoided crossings, with associatively smaller calculated widths and long lifetimes.

Table S4: Resonance stationary points, positions and widths for the Q_{CO}=0.4. The resonance energies, here, are presented in reference to the Coupled Cluster energy at the Q_{CO}=0.4 geometry along α. The resonances parameters are shown for the (3,3,3), (4,4,4), (5,5,5) and (3,3,3,3) GPAs.

	Resonance 1		Resonance 2		Resonance 3	
GPA	Branch Point	Resonance [eV]	Branch Point	Resonance [eV]	Branch Point	Resonance [eV]
(3,3,3)	0.903 ± 0.2392i	0.8498 ± 0.1999i	0.8308 ± 0.1243i	2.202 ± 0.2338i	1.1826 ± 0.163i	3.1615 ± 0.3053i
(4,4,4)	0.8956 ± 0.2357i	0.8464 ± 0.1983i	0.8267 ± 0.127i	2.1988 ± 0.2401i	1.1804 ± 0.1973i	3.1553 ± 0.3315i
(5,5,5)	0.8918 ± 0.2338i	0.8425 ± 0.197i	0.8341 ± 0.129i	2.2106 ± 0.2377i	1.2227 ± 0.1353i	3.2155 ± 0.2899i
(3,3,3,3)	0.8929 ± 0.2347i	0.8432 ± 0.1977i	0.8294 ± 0.1358i	2.203 ± 0.2542i	1.1704 ± 0.1507i	3.1824 ± 0.2824i
(3,3,3)			1.1508 ± 0.0356i	2.4209 ± 0.0600i	1.4651 ± 0.0814i	3.2174 ± 0.1238i
(4,4,4)			1.1522 ± 0.035i	2.4232 ± 0.059i	1.4647 ± 0.0816i	3.2167 ± 0.1241i
(5,5,5)			1.1521 ± 0.0342i	2.4232 ± 0.0577i	1.4375 ± 0.1071i	3.1769 ± 0.1638i
(3,3,3,3)			1.1522 ± 0.0354i	2.4232 ± 0.0597i	1.4619 ± 0.0822i	3.2117 ± 0.1262i
(3,3,3)			1.4271 ± 0.234i	2.4155 ± 0.2712i	1.6651 ± 0.0814i	3.2174 ± 0.1237i
(4,4,4)			1.4417 ± 0.2282i	2.4308 ± 0.2637i	1.6646 ± 0.0818i	3.2165 ± 0.1244i
(5,5,5)			1.436 ± 0.2248i	2.423 ± 0.2583i	-	-
(3,3,3,3)			1.4361 ± 0.2268i	2.4246 ± 0.2601i	1.666 ± 0.0813i	3.2192 ± 0.1231i
(3,3,3)			1.6937 ± 0.3616i	2.3768 ± 0.3851i		
(4,4,4)			1.6932 ± 0.3621i	2.3769 ± 0.3857i		
(5,5,5)			1.6696 ± 0.3614i	2.3496 ± 0.3942i		
(3,3,3,3)			1.6904 ± 0.3628i	2.3739 ± 0.3875i		

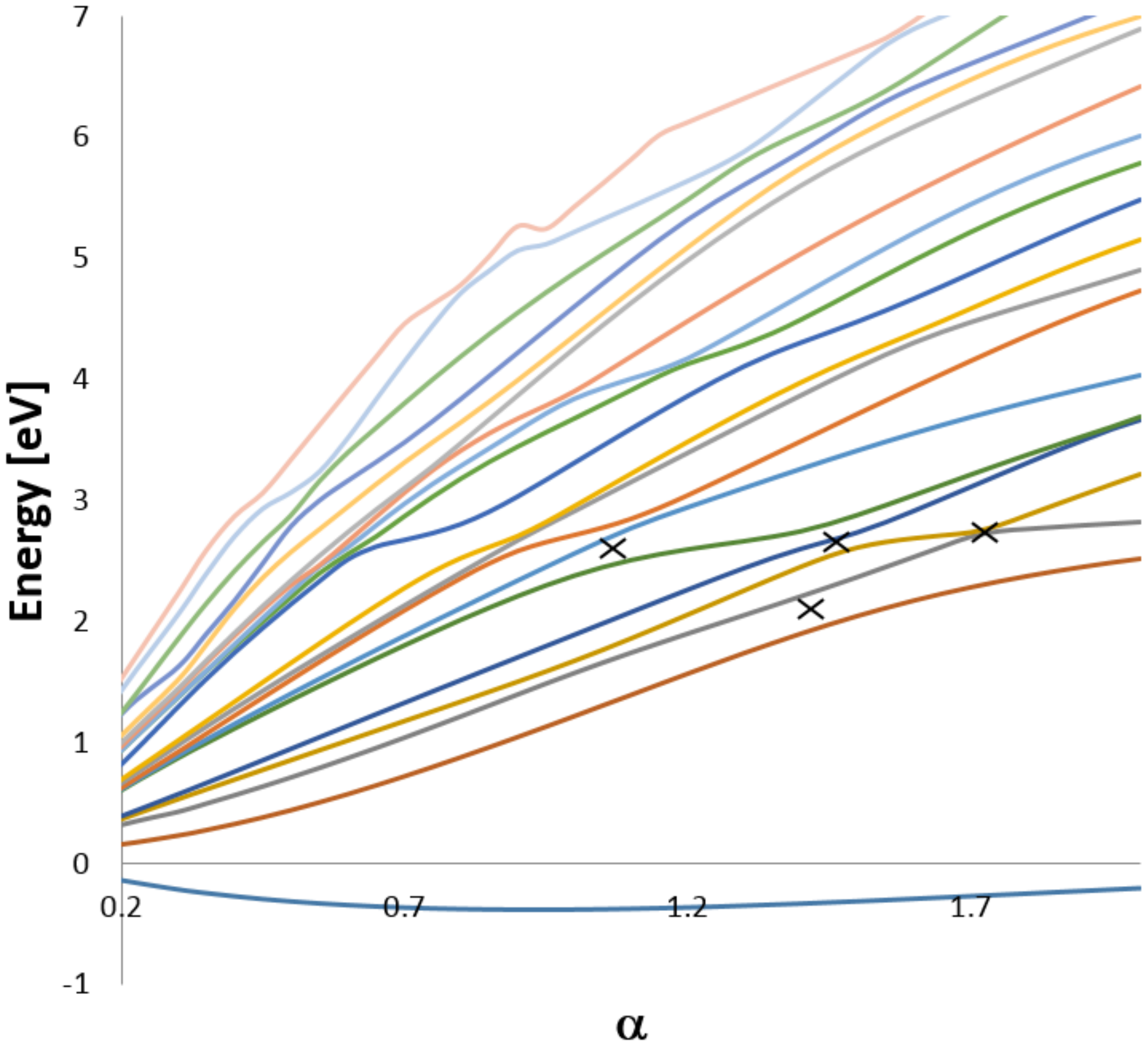

Figure S7: EOM-EA-CCSD/6-31+G* resonance curves for the neutral DFT optimized TS. The first EA is stabilized with respect the CCSD reference and, therefore, exhibits a negative electron attachment energy. Because it is fully bound (not metastable), no resonance parameters need be calculated. By convention, in this work, all **bound** EA and reference energies (i.e. singlet and triplet) are presented at α =1. The 2^2A resonance (~2.16eV) is weakly coupled to the continuum solution. Because of the weakly coupled nature of the second resonance, characterization was aided by tracking the progression of both the 2^2A and 3^2A resonance at lower Q_{CO} values leading into the TS.

Table S5: Resonance branch points, positions and widths are given for the neutral optimized TS (Q_{CO}=0.5). The resonance energies are presented in reference to the coupled cluster reference along each point of α .

	Resonance 1		**Resonance 2**		**Resonance 3**	
GPA	**Branch Point**	**Resonance [eV]**	**Branch Point**	**Resonance [eV]**	**Branch Point**	**Resonance [eV]**
(3,3,3)	Fully Bound		1.4602 ± 0.3351i	2.1777 ± 0.5187i	0.7911 ± 0.1130i	2.6516 ± 0.2064i
(4,4,4)			1.4490 ± 0.3545i	2.1620 ± 0.5500i	0.8047 ± 0.1088i	2.6745 ± 0.2011i
(5,5,5)			1.4503 ± 0.3534i	2.1639 ± 0.5482i	0.806 ± 0.1076i	2.6788 ± 0.1984i
(3,3,3,3)			1.4502 ± 0.3550i	2.1639 ± 0.5505i	0.8054 ± 0.1079i	2.677 ± 0.1991i
(3,3,3)					1.0700 ± 0.1857i	2.6316 ± 0.2215i
(4,4,4)					1.0813 ± 0.1811i	2.6427 ± 0.205i
(5,5,5)					1.0701 ± 0.1814i	2.6286 ± 0.2163i
(3,3,3,3)					1.0543 ± 0.2069i	2.6668 ± 0.2593i
(3,3,3)					1.462 ± 0.1105i	2.7136 ± 0.1734i
(4,4,4)					1.4437 ± 0.1292i	2.6559 ± 0.1533i
(5,5,5)					1.4475 ± 0.1365i	2.6400 ± 0.1784i
(3,3,3,3)					-	-

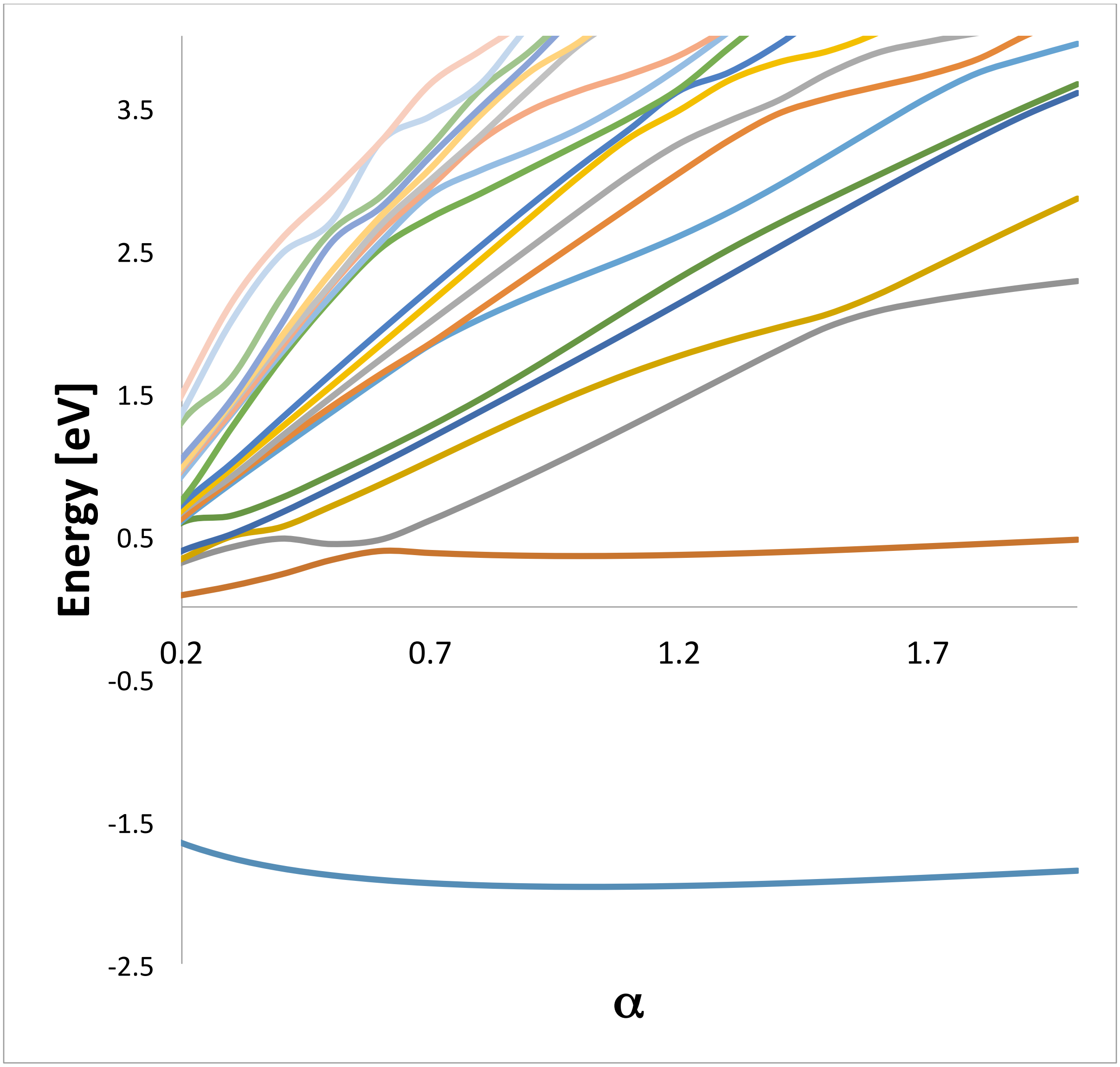

Figure S8: EOM-EA-CCSD/6-31+G* stabilization curve for the anion optimized TS geometry. These calculations illustrate the profound positive EA energy for state 1, which is fully bound due to the open shell nature of the singlet reference electronic configuration.

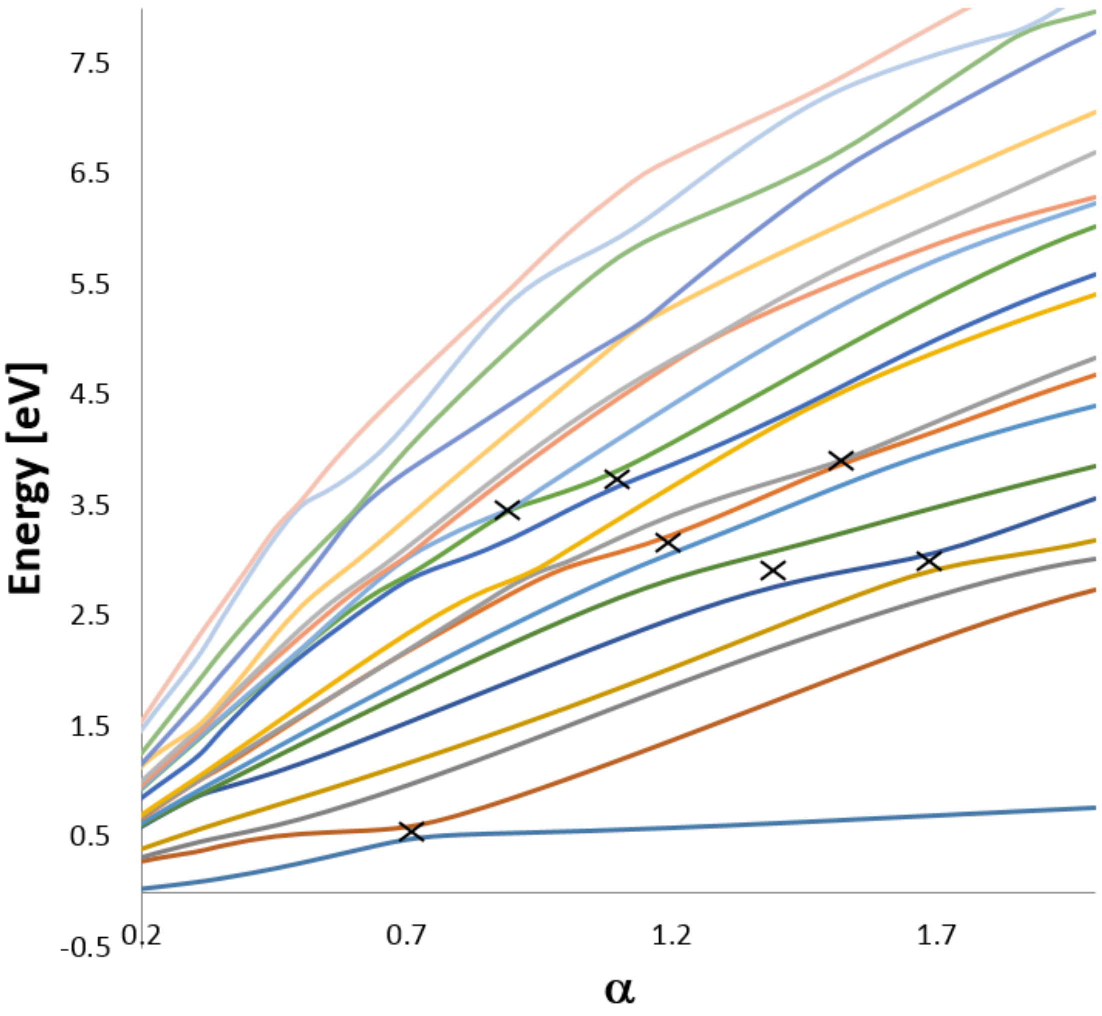

Figure S9: EOM-EA-CCSD/6-31+G* resonance curves for the geometry associated with Q_{CO}=0.6. This configuration shows that following the TS (both neural and anion optimized), the metastable nature of the EA is reconstituted due to the closing of the open shells as the 1,3 dihydroimidazone ring forms and the CO is ejected.

Table S6: Resonance branch points, positions and widths are given for Q_{CO}=0.6. This configuration was included to illustrate that the first resonance is reconstituted (i.e. from bound to metastable again) after the TS configuration. The resonances positions, like the previous examples, are in reference to the coupled cluster energies.

	Resonance 1		**Resonance 2**		**Resonance 3**	
GPA	**Branch Point**	**Resonance [eV]**	**Branch Point**	**Resonance [eV]**	**Branch Point**	**Resonance [eV]**
(3,3,3)	0.7065 ± 0.0807i	0.537 ± 0.0595i	1.1687 ± 0.203i	2.9638 ± 0.3371i	0.8896 ± 0.0033i	3.4522 ± 0.008i
(4,4,4)	0.7064 ± 0.0806i	0.537 ± 0.0594i	1.1673 ± 0.2055i	2.9634 ± 0.3394i	0.8898 ± 0.0043i	3.4528 ± 0.0105i
(5,5,5)	0.7067 ± 0.0802i	0.5371 ± 0.0591i	1.1701 ± 0.2062i	2.9699 ± 0.3404i	0.8899 ± 0.0071i	3.4532 ± 0.0172i
(3,3,3,3)	0.7079 ± 0.0774i	0.5321 ± 0.055i	1.1655 ± 0.202i	2.9671 ± 0.3367i	-	-
(3,3,3)			1.4134 ± 0.2624i	2.9843 ± 0.3047i	1.072 ± 0.1043i	3.6841 ± 0.2185i
(4,4,4)			1.4027 ± 0.2606i	2.9761 ± 0.3053i	1.0744 ± 0.1006i	3.6893 ± 0.2099i
(5,5,5)			1.3966 ± 0.2569i	2.9679 ± 0.302i	1.075 ± 0.1022i	3.6913 ± 0.2143i
(3,3,3,3)			1.3962 ± 0.2611i	2.9681 ± 0.3071i	1.0787 ± 0.1012i	3.6992 ± 0.2118i
(3,3,3)			1.6926 ± 0.1173i	2.9912 ± 0.1443i	1.5231 ± 0.0666i	3.8951 ± 0.1173i
(4,4,4)			1.6923 ± 0.1176i	2.9909 ± 0.1447i	1.5261 ± 0.0689i	3.9003 ± 0.1214i
(5,5,5)			-	-	-	-
(3,3,3,3)			1.6926 ± 0.1176i	2.9913 ± 0.1447i	-	-

3. A brief note on methods used

This section discusses the choices in methods in Figures 5 and 6 of the manuscript. Figure 5 uses the stabilization method combined with EOM-EA-CCSD/6-31+G(d) while Figure 6 uses CASPT2/cc-pVDZ. Figure 6 focuses on a small part of the configuration space covered in Figure 5. The justification for CASPT2 is that a conical intersection is involved, so multireference methods are preferred. On the other hand, a stabilization method should be used when computing resonances – so benchmarks for non-stabilization method derived energies is required. In so doing, computations were undertaken in which an equivalently small 6-31G(d) basis (without diffuse functions) was assigned to the EOM-EA-CCSD method in order to assess the analogous profile explored using CASPT2 along Q_{CO}. The small basis set precludes the requirement for a stabilisation method and negates the relative contamination from continuum states. The returned EOM-EA-CCSD/6-31G(d) profiles are depicted in Fig. S10, and reveal insight into the complexities of the reactive states upon comparisons with the CASPT2 PE profiles. The non-stabilised CASPT2/cc-pVDZ and EOM-EA-CCSD/6-31G(d) PE profiles both clearly identify D_1/D_0 crossings at the approximate geometry of the CASSCF optimised CI - which is itself stable with respect to the neutral closed-shell reference state. This relative stability of the CI substantiates the reliability of the optimised CASSCF D_1/D_0 CI (which was obtained without a stabilisation method). In summary, both CASPT2/cc-pVDZ and EOM-EA-CCSD/6-31G(d) can describe the D_1/D_0 CI adequately. Furthermore, the EOM-EA-CCSD/6-31G(d) curves reveal that at the CI the states are more stable than the neutral system.

When compared to the EOM-EA-CCSD/6-31+G(d) reaction path in Fig. 5 of the manuscript, the CASPT2/cc-pVDZ and EOM-EA-CCSD/6-31G(d) computations show a larger predicted stabilization of the energy for the $3^2\pi^*$ state between Q_{CO} = 0.4 and the optimised TS^-. A plausible explanation for this develops by considering that the geometry at Q_{CO} = 0.4 is poorly described with the small 6-31G(d) basis set since it is metastable - manifesting in a higher energy, while the energy of the CI is described much better by these methods, since the states are not metastable anymore at this point.

Another problem appears when comparing CASPT2/cc-pVDZ and EOM-EA-CCSD/6-31G(d) along the path between Q_{CO} = 0.4 to the CI. We see dramatic differences in the reactivity of the $3^2\pi^*$ state; in the former case the $3^2\pi^*$ state shows a net reaction with respect to nuclear motions from Q_{CO} = 0.4 to the CI whilst the latter shows no reactivity. The reason for the poor description of the EOM-EA-CCSD method can be found in the character of the resonances in this region. The coefficients associated with the CASSCF configuration vectors show heavy mixing between various shape and core-excited shape resonances en route to the CI - as shown by the highlighted configurations in Table S9. The heavily mixed core-excited shape configurations associated with the ultimate reactivity of the D_2 resonance are likely to be poorly described following electron attachment to a closed-shell singlet Ansatz in EOM-EA-CCSD theory. Indeed, we highlighted such a difficultly in our earlier paper - in which a triplet closed-shell Ansatz was used in order to compute the core-excited shape resonances of uracil with EOM-EA-CCSD. We have explored the analogous EOM-EA-CCSD/6-31G(d) path using a triplet reference (see Figure S11). This graph predicts the correct shape for the D_2 state but it cannot describe correctly the lower state. So, this graph too reinforces the multireference nature of the problem - involving states that are heavily mixed as thus poorly described by EOM-EA-CCSD. This can be explained by the lack of versatility of EOM-EA-CCSD, where the only accessible electronic configurations derive from the single placement of an electron to an unoccupied (or partially occupied) MO onto a reference ground state. When the reference configuration is a closed shelled singlet, only π* or σ* occupations are accessible. Similarly, when the reference is a triplet, one may calculate core-excited or valence excited electronic configurations; however, in both cases, EOM-EA-CCSD is unable to determine the contribution of all of these configurations, simultaneously, on a given state as can CASPT2. When combining the two graphs (Figures S10 and S11) in Figure S12 we eventually get all three anion states, but even in this case the mixing between results from different calculations is missing.

The final benchmark involved the computation of the Q_{CI} coordinate using EOM-EE-CCSD - built upon a doublet Hartree-Fock reference wavefunction of the anion. Using this method, the contributions of shape, core-excited and valence excited electronic configurations can be accounted for simultaneously – giving results that agree behaviorally well with our CASPT2 calculations in fig. 5, but the curves are not smooth (see Figure S13). This is occurring because of the conical intersections between the ground and the higher states which changes the character of the doublet reference state. We therefore see that CASPT2 is the best approach in this region, and our combination of EOM-EA-CCSD stabilization curves combined with CASPT2 when necessary is the most appropriate way to describe this problem.

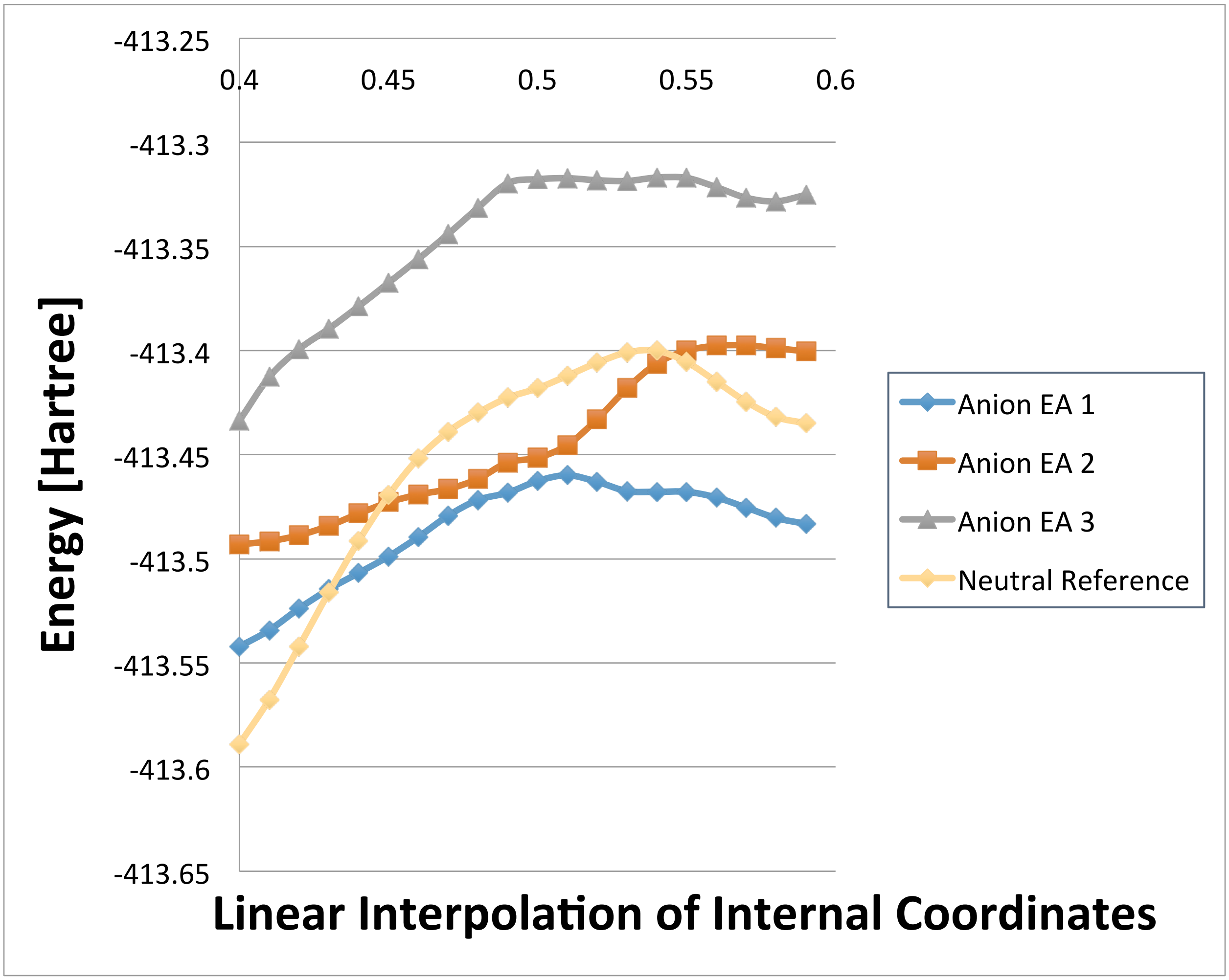

Figure S10: EOM-EA-CCSD/6-31G* linear interpolation from Q_{CO}=0.4 through the D_0/D_1 CI to the neutral TS. The EOM-EA-CCSD calculations were performed on each geometry using a neutral singlet reference in C1 symmetry. No diffuse functions were used to avoid the formation of continuum states.

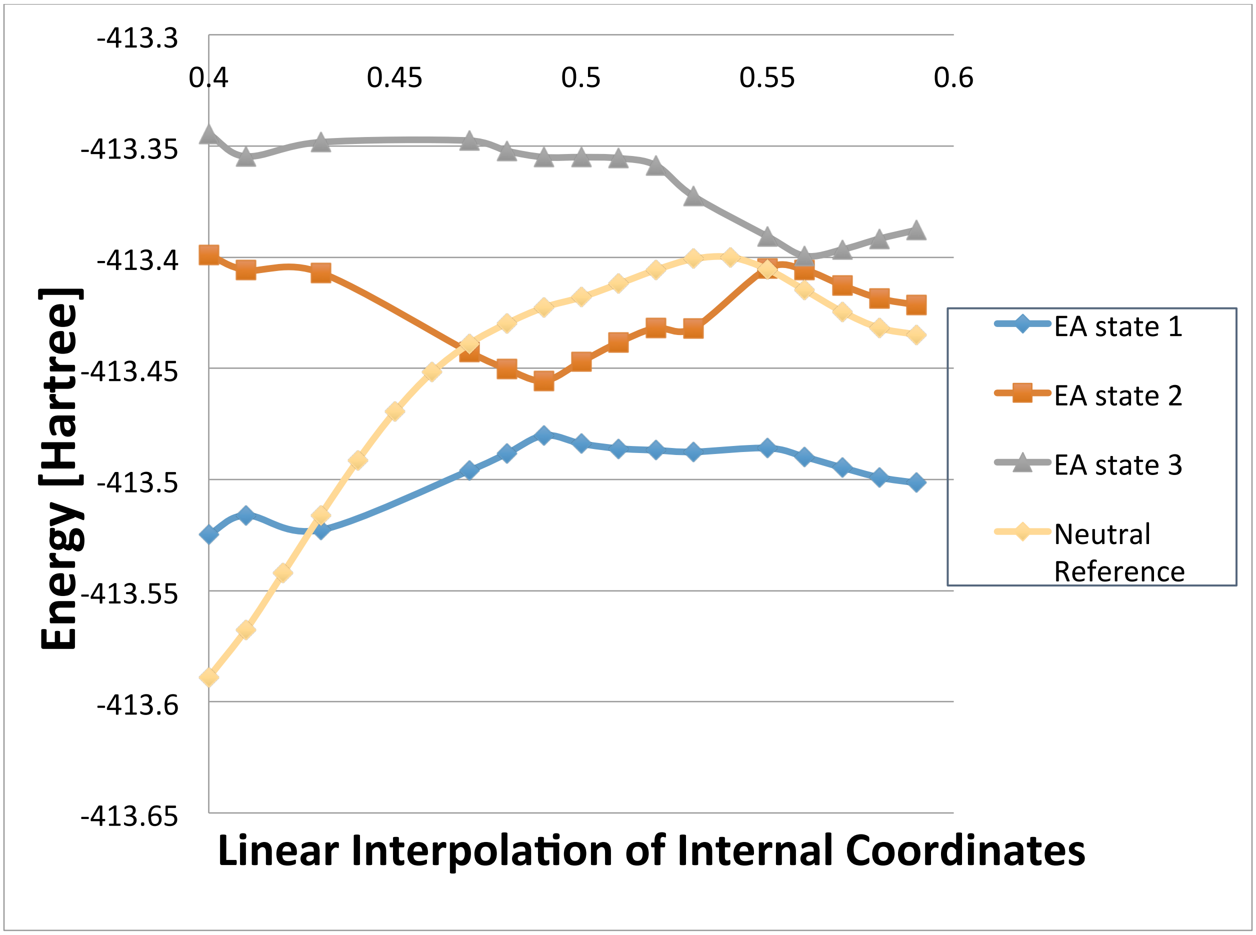

Figure S11: EOM-EA-CCSD/6-31G* linear interpolation from Q_{CO}=0.4 through the D_0/D_1 CI to the neutral TS. Similar to the preceding example (Figure S10), EOM-EA-CCSD calculations were performed at each geometric step but – this time – using a triplet reference configuration.

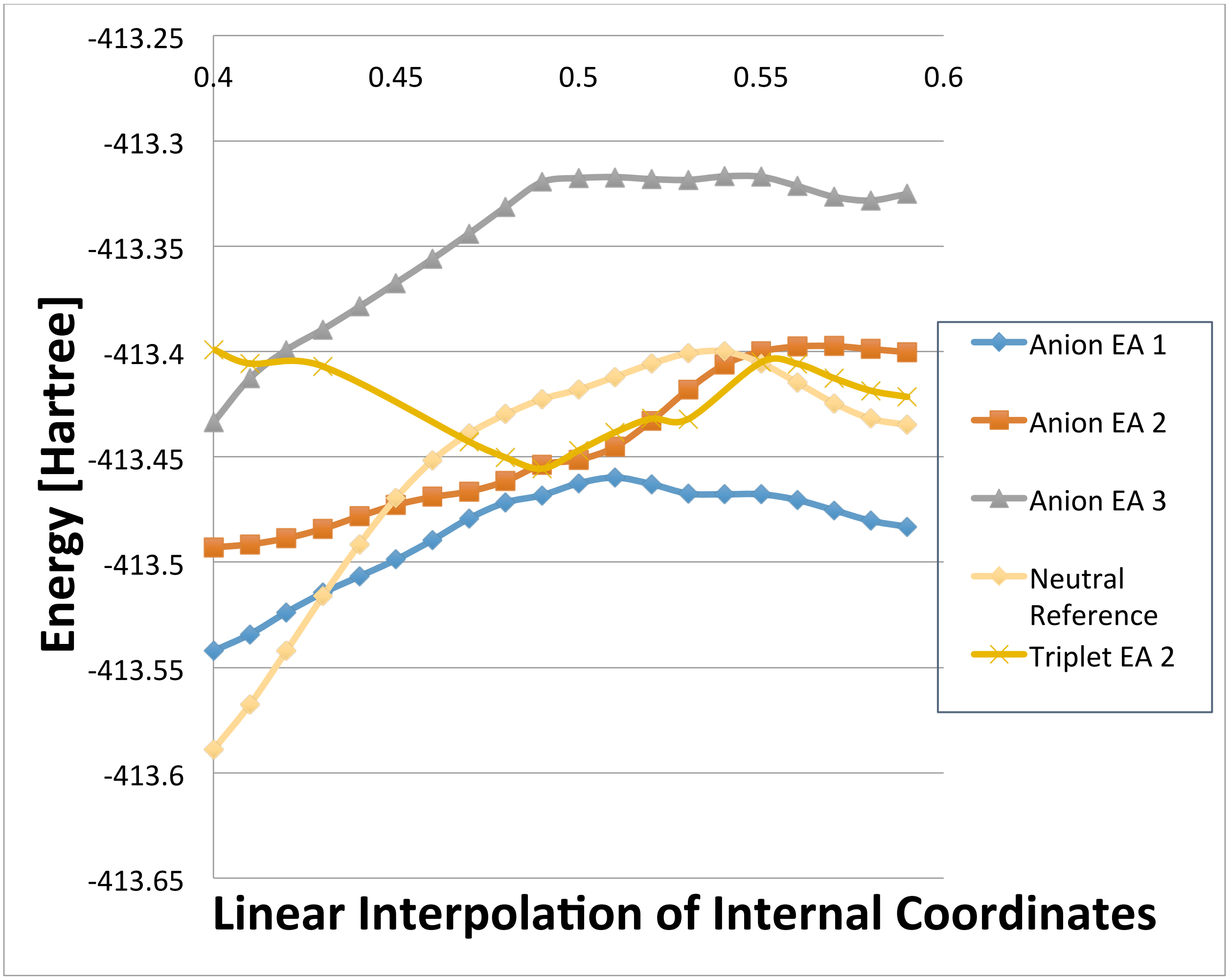

Figure S12: Composite between Figures S10 and S11. The electron attachment energies associated with both singlet and triplet reference configurations show that the 2^2A (Triplet reference) EA has predominantly core-excited character (amplitude 0.9339) – resulting in behavior similar to the 3^2A in our CASPT2 results. When we compare the 2^2A (triplet reference) resonance with the 3^2A (singlet reference), it becomes clear that a proper description of the third resonance near the D_0/D_1 CI would likely include core-excited character.

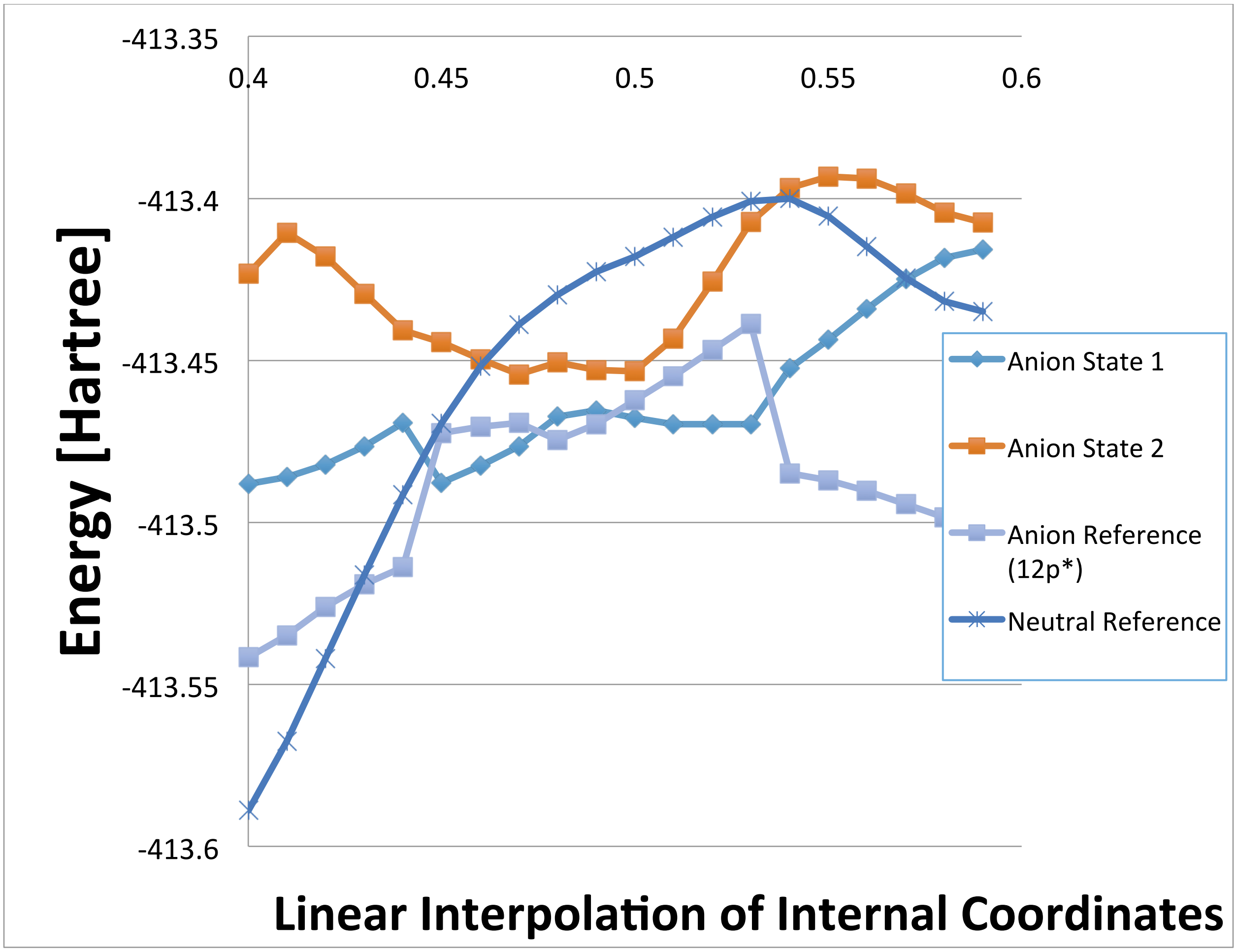

Figure S13: EOM-EE-CCSD/6-31G* linear interpolation from Q_{CO}=0.4 through the D_1/D_0 CI to the neutral TS using anion reference starting configurations.

Table S7: EOM-EE-CCSD/6-31+G* amplitudes and electronic configurations associated with the Q_{CO}=0.4 geometry. At this geometry, electronic configurations characteristic of shape resonances dominate the description of the first 4 electronic excitations – with a core-excited configuration (EE State 4) appearing at higher energies. This picture is consistent with that shown in the body of our work (ref Paper Figure 4). The electronic configurations are shown from orbital 28-34. The characters 0, 2, a and b represent electronic configurations consistent with molecular orbitals that are unoccupied, doubly occupied, singly occupied (spin up) and singly occupied (spin down) respectively.

Q_{CO}=0.4	**Amplitudes**	**Electronic Configuration**	**Characterization**
GS	(Anion Ref)	22a0000	Shape
EE State 1	0.9397	220a000	Shape
EE State 2	0.8347	22000a0	Shape
EE State 3	0.9878	2000a00	Shape
EE State 4	0.6918	2a20000	Core-Excited

Table S8: EOM-EE-CCSD/6-31+G* amplitudes and electronic configurations associated with the D_1/D_2 CASPT2 conical intersection. The electronic configuration (below) highlight the appropriateness of using CASPT2 due to the significant contributions of shape, core-excited and so-called valence excited configurations simultaneously in the description of all three states of interest. These results agree qualitatively well with our CASPT2 description of the D_2/D_1 CI.

CI Geo	**Amplitudes**	**Electronic Configuration**	**Characterization**
GS	(Anion Ref)	22a0000	Shape
EE State 1	-0.5444	2baa000	Valence Excited
	-0.4351	220a000	Shape
	-0.4056	a220000	Core-Excited
EE State 2	-0.7033	a220000	Core-Excited
	0.3341	2baa000	Valence Excited
	0.315	220a000	Shape
EE State 3	0.7428	220a000	Shape
	0.4808	b2aa000	Core-Valence-Excited
	-0.2563	2baa000	Valence Excited

Table S9: Most probable CASSCF CI coefficients associated with the various electronic states of the uracil anion at selected points along the CASPT2 PE profiles depicted in fig. 6. The first column represents the most probably permutations of the active orbital electronic configurations in which 2, 0 and a/b represent doubly occupied, completely unoccupied and singly occupied orbitals. The second, third, fourth and fifth columns represent, respectively the D_0, D_1, D_2, D_3 states, within which the numbers represent the CI coefficients which indicate the weight contribution of a particular electronic configuration.

Point 1

2222200a00	0.1725763	-0.0443738	-0.0433311	0.8761590	0.2958990
22222a0000	0.8244946	-0.4126402	-0.2266178	-0.1615938	-0.0560547
22222000a0	-0.2054514	-0.4580720	0.0709414	-0.2375478	0.7576750
222220000a	-0.0608157	-0.5136843	0.7017435	0.1369460	-0.3424357
222220a000	0.4218369	0.5099160	0.5929123	-0.1389409	0.3221422
2222020a00	-0.0513248	0.0181749	0.0138363	-0.1570399	-0.0532365
22220200a0	0.0339614	0.0852029	-0.0108060	0.0448542	-0.1390056
222202000a	0.0090131	0.0894744	-0.1194178	-0.0231915	0.0586621
222202a000	-0.1074036	-0.0796132	-0.1015070	0.0300812	-0.0584902
2220202a00	-0.0010075	0.0283872	0.0311612	-0.1067372	-0.0198866
22202020a0	0.0273624	0.0597204	-0.0037074	0.0268839	-0.0896877
2222ab00a0	0.0059445	0.0304788	0.0402653	0.0410061	-0.0883534
222020200a	0.0081099	0.0637627	-0.0843183	-0.0171873	0.0427437
2222a20000	-0.0273472	0.0249003	0.0206656	0.0795385	0.0730871
2222ba00a0	-0.0095334	-0.0136546	-0.0190239	-0.0204158	0.0764001

Point 2

22222000a0	-0.0069668	0.2654307	0.9035646	-0.0868346	-0.0594130
22222a0000	0.8799372	0.3556696	-0.0823186	0.0711290	0.1466493
2222200a00	-0.0061061	-0.2374923	0.1715204	0.8379314	0.2967942
222220a000	-0.3767610	0.8003663	-0.2024806	0.1858922	0.2139294
2222a20000	-0.0076914	-0.1239192	0.0605123	-0.3173205	0.6937974
2222a02000	0.0020750	0.0966274	-0.0446702	0.1611920	-0.3426743
2222baa000	-0.0890105	-0.0365576	-0.0017515	-0.0995268	0.3321830
2222aab000	0.0210285	0.0605614	-0.0294318	0.0828791	-0.2327967
222202a000	0.1337366	-0.0889152	0.0255539	-0.0270797	-0.0023974
22220200a0	-0.0009678	-0.0353441	-0.1181747	0.0127777	0.0012825
2222020a00	0.0141411	0.0411584	-0.0263141	-0.1140641	-0.0518835
2222aba000	0.0679820	-0.0240037	0.0311833	0.0166476	-0.0993864
22220a2000	-0.0992453	0.0479085	-0.0129022	0.0035853	0.0323913
22202002a0	0.0016580	-0.0252316	-0.0905522	0.0048354	0.0047678

Point 3

22222000a0	-0.0151324	-0.1360491	0.9063764	0.0965765	0.1395802
22222a0000	0.8506414	-0.3814506	-0.0163855	0.0269078	-0.2108155

222220a000	0.4080585	0.7944610	0.0764836	0.0070214	0.2910546
2222200a00	0.0359919	-0.2510455	-0.2011839	0.5515106	0.6635391
2222a20000	-0.0241758	0.1833482	0.0297646	0.6057162	-0.3591264
2222a02000	-0.0055722	-0.1129703	-0.0286963	-0.3365036	0.2552596
2222baa000	0.0899796	-0.0600049	0.0087352	-0.2650606	0.2437495
2222aab000	-0.0121298	0.0516863	0.0190913	0.1770901	-0.1940841
222202a000	-0.1457235	-0.0884812	-0.0132214	-0.0167571	-0.0111500
22220200a0	-0.0006435	0.0192233	-0.1215594	-0.0165300	-0.0137517
22220a2000	-0.1124372	-0.0476764	-0.0077766	0.0152418	-0.0240122
2222020a00	-0.0180230	0.0433381	0.0305483	-0.0789175	-0.1040608
2222aba000	-0.0778499	0.0083186	-0.0278265	0.0879705	-0.0496655
22220ab0a0	0.0011600	-0.0138025	0.0833140	0.0083581	0.0122256

Point 4

222220a000	0.8071725	-0.4624937	0.1154490	0.0524765	-0.0336107
22222a0000	0.4503629	0.7649397	-0.1713200	0.2003328	-0.1847416
2222200a00	-0.1790213	-0.0909640	0.3842323	0.7492277	-0.3199902
2222a20000	0.0771553	0.1755047	0.2753700	0.2139489	0.7258158
2222aab000	0.0282940	0.1776195	0.6199823	-0.3599447	-0.1730186
2222aba000	0.0029373	-0.0831064	-0.3190980	0.1833554	0.0610090
2222baa000	-0.0312314	-0.0945131	-0.3008843	0.1765893	0.1120096
2222aa0b00	-0.0026429	-0.0490896	-0.1238966	-0.0987863	-0.2906093
2222ba0a00	0.0255978	0.0581650	0.0892074	0.0625530	0.2097572
222202a000	-0.1802164	0.1032974	-0.0202109	-0.0218301	-0.0018154
2222a0ba00	-0.0147463	-0.0561190	-0.1795334	0.0996352	0.0362909
2222a00200	-0.0113206	-0.0441952	-0.0723769	-0.0613719	-0.1736087
2222020a00	0.0705451	0.0722038	-0.1017601	-0.1568303	0.0649225
2222a0ab00	0.0109348	0.0265941	0.0990200	-0.0514726	-0.0122526
2222ab0a00	-0.0229549	-0.0090754	0.0346892	0.0362334	0.0808521

Point 5

222220a000	0.8493072	0.3422834	0.1053427	0.0757484	-0.0346991

22222a0000	-0.3302015	0.7836163	0.2307226	-0.0785492	0.2709998
2222200a00	-0.1633872	0.1092629	0.2621983	0.7007926	-0.4232091
2222aab000	0.0141956	-0.1964176	0.6679191	-0.2503771	-0.0787026
2222a20000	-0.0723091	0.2461577	-0.1342157	-0.4163006	-0.6326308
2222aba000	0.0169960	0.0984032	-0.3418529	0.1482050	-0.0493980
2222baa000	-0.0311916	0.0980144	-0.3260662	0.1021721	0.1281006
222b2aa000	-0.0134362	-0.0411434	-0.0470618	0.0829157	-0.2188341
2222aa0b00	-0.0020894	0.0680830	-0.0927692	-0.1971621	-0.2148263
2222a0ba00	0.0109705	-0.0697435	0.2125291	-0.0810324	-0.0088782
222202a000	-0.1981160	-0.0846371	-0.0185204	-0.0296975	0.0224177
2222020a00	0.0626596	-0.0821723	-0.0855205	-0.1720327	0.0795911
2222ba0a00	0.0215565	-0.0855950	0.0559138	0.1301317	0.1628720
222a2ab000	0.0016056	0.0369546	0.0425495	-0.0533286	0.1593945
2222a00200	0.0145475	-0.0725107	0.0499283	0.1256003	0.1562477
2222a0ab00	-0.0194779	0.0264856	-0.1149272	0.0339002	-0.0018091
22022a2000	0.0110665	-0.0999314	-0.0483922	0.0039595	-0.0141093

Point 6

222220a000	0.8350383	0.1437445	0.0769233	0.0249989	0.2642904
22222a0000	-0.1636886	0.7903072	0.3208592	0.0074048	0.0109176
2222aab000	-0.0099230	-0.2787153	0.6709539	-0.0676058	-0.0045571
2222200a00	-0.0699330	0.0979181	0.1007732	0.6666775	0.0060599
2222baa000	-0.2402683	0.1055328	-0.3425383	-0.0196029	0.4679365
2222aba000	0.2501913	0.1731825	-0.3284155	0.0872087	-0.4633795
222a2ba000	-0.0390985	-0.0274094	0.0550040	0.0364685	-0.4607595
2222a20000	-0.0164726	0.2179765	0.0303967	-0.4186475	-0.1187800
222b2aa000	0.0381266	0.0133111	0.1044782	-0.0508831	0.3400312
2222ab0a00	-0.0286202	0.0520549	0.0439640	0.3039974	0.0223407
2222aa0b00	-0.0001307	0.0850876	0.0036798	-0.2800335	-0.0390576
2222020a00	0.0230659	-0.0463309	-0.0403052	-0.1987061	-0.0109483
2222a0ba00	0.0015563	-0.0846411	0.1861822	-0.0159501	0.0104538
222202a000	-0.1830548	-0.0371591	-0.0132697	-0.0228381	0.0991961
222a2ab000	0.0009719	0.0140983	-0.1594822	0.0144146	0.1207283
2222ba0a00	0.0287508	-0.1371425	-0.0476438	-0.0239638	0.0167169
2222a00200	0.0063968	-0.0892117	-0.0168745	0.1355196	0.0252637
22022a2000	0.0077310	-0.1174658	-0.0657727	-0.0054161	0.0116841
222a220000	0.0149024	-0.1171634	-0.0317569	0.0933767	0.0035031
2202202a00	-0.0078985	-0.0270489	-0.0187607	-0.1103830	-0.0041129

Point 7

22222a0000	-0.2381563	-0.1141666	0.8445813	-0.1705388	0.1514664
222220a000	0.6807102	0.0510185	0.2765669	0.5146048	0.0113227
2222aab000	-0.0282203	0.6715392	0.0686110	-0.0648940	0.1592655
222a2ab000	0.0068398	-0.1295056	-0.1748520	-0.0100493	0.6334241
2222baa000	-0.3842268	-0.4003589	-0.0385786	0.5306335	-0.0858935
2222aba000	0.4124471	-0.2711802	-0.0300325	-0.4657394	-0.0733720
222a2ba000	-0.1156457	0.0507789	0.0244646	-0.1148507	-0.3542578
222a220000	-0.0364268	0.0747053	-0.0433759	-0.0426493	-0.3282084
2222a20000	0.1398918	-0.3126834	0.0557345	-0.1465619	-0.0169792
222a202000	0.0581502	-0.0563748	-0.0475821	0.0717039	0.3065674
2222a02000	-0.1405038	0.2914959	0.0132276	0.1295922	0.0573925
222b2aa000	0.1088059	0.0787267	0.1503874	0.1249000	-0.2791663
2222ba0a00	-0.0018381	-0.0240226	0.1381315	-0.0051228	0.0361542
2222aa0b00	-0.0120591	0.0191356	-0.1244779	0.0014446	-0.0441549
22220a0200	0.0137449	0.0115554	-0.1061382	0.0204000	-0.0249382
22220aba00	0.0026929	-0.1000883	-0.0172762	0.0108853	0.0177304
2222200a00	0.0181139	0.0072743	-0.0998102	0.0004617	-0.0537085

Point 8

22222a0000	-0.0995910	0.1618500	0.8649462	-0.2134386	0.0767967
222220a000	0.2809003	0.1786873	0.1786977	0.8025629	0.0304146
222a2ab000	0.0149731	-0.0806473	-0.0853655	-0.0530068	0.6192153
2222aba000	0.5969448	-0.0246377	0.0128110	-0.1981481	-0.0325738
2222aab000	-0.1456785	0.5919125	-0.1352471	-0.0480672	0.0656759
2222baa000	-0.4512663	-0.5672747	0.1224362	0.2462153	-0.0331022
222a220000	-0.0379185	0.0115651	-0.0729366	-0.0843981	-0.4173079
222a202000	0.0375508	-0.0363465	-0.0407048	0.0820098	0.3857312
222b2aa000	0.0477142	0.0704089	0.0391965	0.2394906	-0.3744109
2222a20000	0.3465777	-0.2813776	0.1102589	-0.0682995	-0.0328332
2222a02000	-0.3350392	0.2779952	-0.0727551	0.0701003	0.0402260
222a2ba000	-0.0626872	0.0102384	0.0461690	-0.1864837	-0.2448044
2222ba0a00	0.0104846	0.0272917	0.1799597	0.0299834	0.0292549
2222aa0b00	-0.0028668	-0.0356773	-0.1752761	-0.0448707	-0.0343010
22220a0200	0.0038292	-0.0237231	-0.1440653	0.0069667	-0.0168736
222022a000	-0.0246393	-0.0101739	-0.0008027	-0.1126381	0.0077697
22220aba00	0.0218824	-0.0947704	0.0208531	0.0103528	-0.0008730
22220aab00	0.0694357	0.0933632	-0.0183601	-0.0294068	0.0007461
22220baa00	-0.0913182	0.0014072	-0.0024930	0.0190540	0.0001269
222ba2a000	0.0899877	-0.0151052	0.0042680	-0.0429390	0.0125140

4. Cartesian coordinates [in Angstrom] for structures in Figure 3

Structure 1:

N	-0.043772000000	1.056823000000	-0.048618000000
C	-1.384244000000	0.660084000000	0.023286000000
H	-2.209074000000	1.357324000000	-0.023091000000
C	-1.328412000000	-0.708480000000	0.013184000000
H	-2.172288000000	-1.390933000000	0.008940000000
N	-0.038945000000	-1.183947000000	-0.009438000000
C	0.779680000000	-0.096324000000	-0.011568000000
O	2.029586000000	-0.022846000000	0.015834000000
H	0.321549000000	1.974570000000	0.144460000000

Structure 2A:

N	1.289768000000	-0.689536000000	-0.079389000000
C	1.357096000000	0.679107000000	0.010650000000
H	2.314167000000	1.190211000000	0.015832000000
C	0.077469000000	1.151342000000	0.009427000000
H	-0.248492000000	2.182803000000	-0.019277000000
C	-0.813407000000	-0.024815000000	0.007053000000
O	-2.075792000000	-0.009418000000	0.003977000000
N	-0.028019000000	-1.145148000000	0.002681000000
H	1.981473000000	-1.288685000000	0.345808000000

Structure 2B:

N	-1.382592000000	-0.768697000000	-0.000002000000
C	-1.421465000000	0.563928000000	0.000001000000
H	-2.391411000000	1.053649000000	0.000003000000
C	-0.149703000000	1.165599000000	-0.000001000000
H	0.093519000000	2.219094000000	0.000000000000
C	0.800703000000	0.098220000000	-0.000001000000
O	2.060063000000	0.040393000000	0.000000000000
N	-0.026148000000	-1.028794000000	0.000001000000
H	0.301356000000	-1.979921000000	0.000004000000

Structure 3A:

N	-2.180510000000	-0.068997000000	-0.140294000000
C	-0.814970000000	0.018416000000	0.015390000000
H	-2.701281000000	0.697205000000	0.261785000000

C	0.089480000000	1.125042000000	0.154410000000
H	0.093161000000	2.055860000000	-0.412600000000
C	1.069645000000	0.008702000000	0.038288000000
O	2.274316000000	-0.124415000000	-0.078909000000
N	0.024131000000	-1.029623000000	0.061154000000
H	-2.556692000000	-0.980362000000	0.087533000000

Structure 3B:

N	-2.256383000000	-0.158422000000	0.051209000000
C	-0.984036000000	0.045593000000	-0.030732000000
H	-2.725751000000	0.743664000000	0.159942000000
C	0.014019000000	1.078036000000	-0.004974000000
H	-0.000525000000	2.155682000000	-0.106239000000
C	1.031358000000	0.087712000000	-0.014913000000
O	2.249490000000	-0.037383000000	0.065291000000
N	0.020904000000	-1.006569000000	-0.170976000000
H	0.010668000000	-1.713391000000	0.566053000000

[1] K. D. Jordan, Chem. Phys., 1975, **9**, 199.

[2] K. D. Jordan, J. Mol. Spectrosc., 1975, **56**, 329–331.

[3] L. Yu and J. S.-Y. Chao, J. Chin. Chem. Soc., 1993, **40**, 11–22.